Meteorol. Z. (Contrib. Atm. Sci.), Vol. **30**, No. 3, 271–278 (published online March 26, 2021)

Boundary-Layer Meteorology

On the importance of a viscous surface layer to describe the lower boundary condition for temperature

Günter Gross*

Institut für Meteorologie und Klimatologie, Leibniz Universität Hannover, Germany

(Manuscript received January 9, 2021; in revised form February 27, 2021; accepted March 1, 2021)

Abstract

A viscous sublayer was introduced into a PBL model in order to specify the lower boundary condition for temperature. The simulated results have been compared against available observations. However, for such a comparison, some of the variables and parameters that are necessary are not known but can be deduced from observed data. In this way, surface temperature and thermal diffusivity of the soil, representative for the four-day period studied here, have been estimated from measured data. An optimized relation for the thickness of the viscous sublayer δ was found that includes the diurnal variation of the properties of the air flow. Including this approach in the model, simulated temperatures in the ground at different levels as well as temperature in the atmosphere agree very well with the observations. The applicability for a wider range of wind speeds was demonstrated by calculating daily maximum temperatures $T_{\max}$. An analysis of long-term observations for the summer season at different operational weather stations consistently show a distinct maximum of $T_{\max}$ for a 10-m wind between 2–3 m/s, which can be explained by the interaction between the molecular transport of heat within the viscous sublayer of thickness δ and the turbulent heat flux.

Keywords: Boundary layer model, surface temperature, viscous sublayer

1 Introduction

To describe atmospheric processes by a numerical model, the lower boundary conditions for the meteorological variables in particular need to be specified. Based on many research papers on the planetary boundary layer (PBL), it is well established that the vertical profiles of the variables follow a logarithmic law. Since this log-function is not defined at height $z = 0$, a small length scale z_o is introduced where the lower boundary conditions are defined. The roughness length z_o can be estimated from surface features (Garratt, 1992) and this concept can be applied with great success for momentum with the wind speed equal to zero at $z = z_o$. However, temperature at this height is not known; instead, it is usually very close to the ground temperature. Information about the surface radiation (or skin) temperature T_o is available. T_o may be observed or calculated by a surface energy balance equation. To formulate a lower boundary condition, Deardorff (1974) gives an expression to relate this surface temperature to the temperature at height $z = z_o$ (see Eq. (2.9)).

The near surface temperature is an essential parameter to estimate the sensible surface heat flux close to the ground and therefore the energy transfer from the surface into the boundary layer. However, using the radiation temperature instead of the aerodynamic surface temperature at a roughness height (T_1) may result in significant errors in calculating the sensible heat flux. Evaluating Cabauw data, Beljaars and Holtslag (1991) found temperature differences between T_o and T_1 of up to ±6 K for different thermal stratifications. Such large temperature gradients occur in a very thin layer with a thickness on the order of millimeters adjacent to the surface. Inside this viscous sublayer, molecular processes are primarily responsible for heat and moisture transfer up to a height where turbulence takes over the transport (Garratt, 1992; Sun et al., 1995). The effects of such a viscous sublayer in general have been incorporated into numerical models and it was shown that this inclusion can improve model results through a better representation of the sensible heat flux (Liu et al., 1979; Janjic, 1994; Chen et al., 1997).

One approach to describe and to calculate sensible heat flux in the lower part of the atmosphere is the introduction of a thermal roughness length for temperature z_{oT}, which differs from the z_o for momentum (Mahrt, 1996; Zeng and Dickinson, 1998). A reasonable justification to distinguish between these two different roughness lengths derives in particular from the fact that the transfer of heat and momentum from the ground into the adjacent air is controlled by different physical mechanisms. While form drag determines momentum flux, heat flux is due nearly completely to heat conduction.

Although the idea to use different roughness lengths for heat and for momentum is supported by observations (Chen et al., 1997), general guidance on how to estimate z_{oT} is not available (Zeng and Dickinson, 1998).

A common finding is that the thermal roughness length is usually smaller than the roughness length for

*Corresponding author: Günter Gross, Institut für Meteorologie und Klimatologie, Leibniz Universität Hannover, Herrenhäuser Str. 2, 30419 Hannover, Germany, e-mail: gross@muk.uni-hannover.de

DOI 10.1127/metz/2021/1073
Gebrüder Borntraeger Science Publishers, Stuttgart, www.borntraeger-cramer.com

momentum and a simple approach is to describe z_{oT} as a fixed fraction of z_o. Garratt (1992) gives an approximation for the roughness length relation of $z_{oT} \approx z_o/10$, while Beljaars and Holtslag (1991) reported a much smaller value of z_{oT}. However, it is reasonable to assume that a fixed ratio does not cover the broad range of atmospheric situations. As a practical approach, Zilitinkevich (1995) published a relation for z_{oT}/z_o that includes the properties of the air flow. This relation was applied by Chen et al. (1997), and in comparisons with observations, they found better results for the surface heat flux and radiation temperature simulations.

As an alternative approach, Janjic (1994, 2019) introduced the thickness of the viscous sublayer δ into a weather prediction model to define a lower boundary condition for temperature for the turbulent atmosphere above. This value, T_1, is expressed as a weighted mean of temperatures at the surface and the lower atmosphere, observed or modelled. The idea of using δ has earlier been used by Liu et al. (1979) to estimate the air-sea exchange of heat.

In this paper, it is shown that the concept of a viscous sublayer, introduced into a high resolution PBL model, is an important link between the surface and the atmosphere close to the ground, and in particular, it is important to formulate the lower boundary condition for temperature by taking into account the thickness δ.

2 Theoretical aspects

2.1 Heat energy budget and viscous sublayer

The temperature at the surface can be determined by a surface energy budget, which includes the sensible and latent heat flux ($Q_{H,m}$ and $Q_{V,m}$) and heat transfer in the underlying soil material (Q_G) as well as net long-wave ($Q_L + Q_{L\downarrow}$) and short-wave radiation (Q_S).

Equations and notations are conventional (e.g., Stull, 1988) or given in Fig. 1, and the surface heat budget reads

$$Q_S + Q_{V,m} + Q_{H,m} + Q_L + Q_{L\downarrow} + Q_G = 0 \qquad (2.1)$$

A positive sign is used for the energy gain of the surface, and a negative sign is used for energy loss. Short-wave radiation is either given by observations or is calculated by

$$Q_S = (1 - a) I \sin(h) \qquad (2.2)$$

with albedo (a), solar irradiance (I) and zenith angle (h), depending on the location and time.

For the net outgoing long-wave radiation, the outgoing part is calculated according to the Stefan–Boltzmann law:

$$Q_L = \varepsilon \sigma T_o^4 \qquad (2.3)$$

where the surface emissivity (ε) as well as the downward directed long-wave radiation flux ($Q_{L\downarrow}$) need to be

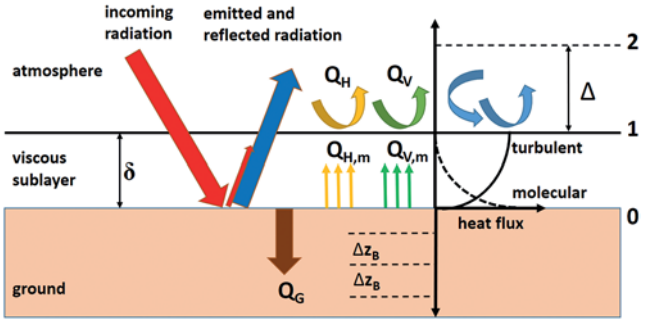

Figure 1: Schematic view of the heat budget in the viscous sublayer.

considered. Flux-gradient relationships have been used to determine the latent and sensible heat flux within the viscous sublayer of depth δ:

$$Q_{H,m} = c_p \rho \nu_h \frac{\partial T}{\partial z} = c_p \rho \nu_h \frac{T_1 - T_o}{\delta} \qquad (2.4)$$

$$Q_{V,m} = L \rho \nu_q \frac{\partial q}{\partial z} = L \rho \nu_q \frac{q_1 - q_o}{\delta} \qquad (2.5)$$

q is the specific humidity, ν_h and ν_q are the molecular diffusivities of heat and moisture ($\nu_h = 2.1 \cdot 10^{-5}$ m^2 s^{-1}, $\nu_q = 2.5 \cdot 10^{-5}$ m^2 s^{-1}, Garratt, 1992), c_p and L are the specific and latent heat and ρ is the air density.

The heat flux into or out of the soil, Q_G, is calculated for different locations inside the ground (Δz_B is the thickness of the first inner layer, see Fig. 1) with thermal conductivity λ by

$$Q_G = \lambda \frac{\partial T}{\partial z} = \lambda \frac{T_o - T_B}{\Delta z_B} \qquad (2.6)$$

while for the temperature inside the material, T_B, the heat conduction equation

$$\frac{\partial T_B}{\partial t} = \nu_B \frac{\partial^2 T_B}{\partial z_B^2} \qquad (2.7)$$

with thermal diffusivity ν_B is used.

Molecular processes are primarily responsible for the transfer of sensible heat and humidity from the land surface to the air above. Within this viscous sublayer, vertical transports are determined entirely by molecular diffusion. Above this thin layer of thickness δ on the order of millimeters, turbulence takes over to transport the properties of air to higher levels of the atmosphere. To determine such turbulent fluxes, e.g., by flux-gradient relationships, the values of temperature and humidity at the top of this viscous sublayer must be known. According to Stull (1988), molecular heat flux in the lowest sublayer and turbulent transport in the upper part must be the same. Assuming flux gradient relationships, this reads

$$\begin{aligned} \nu_h \frac{T_1 - T_o}{\delta} &= K \frac{T_2 - T_1}{\Delta} \\ \Rightarrow T_1 = \frac{T_o + a T_2}{1 + a} \quad &\text{with} \quad a = \frac{K \delta}{\nu_h \Delta} \end{aligned} \qquad (2.8)$$

Table 1: Selected values of the parameter A from literature.

Author	assumptions	A
Schlichting and Gersten (1997)		5
Garratt (1992)		$A = 5$–30
Chriss and Caldwell (1984)		$A = 9$–25
Gross	see below	$A = 19.2$
Janjic (1994)	$M = 10$, $z_o = 0.01$ m, $u_* = 0.1$ m/s	$A = 10$
	$M = 30$, $z_o = 0.03$ m, $u_* = 0.3$ m/s	$A = 51$
Deardorff (1974)	$z_o = 0.01$ m, $u_* = 0.1$ m/s	$A = 0.8$
	$z_o = 0.03$ m, $u_* = 0.3$ m/s	$A = 2.1$

with eddy diffusivity K and Δ is the thickness of the first layer in the atmosphere (see Fig. 1).

The lower boundary condition for temperature in the turbulent layer, T_1, is expressed as a weighted mean of the values at the surface (T_o) and the observation level or the lowest level of a model (T_2). A similar type of equation can be derived when the estimates of Deardorff (1974) or Pielke (2002) are used.

$$\begin{aligned} T_1 &= T_o - 0.74\frac{\overline{w'\vartheta'}}{\kappa u_*}0.13\left(\frac{u_* z_o}{\nu}\right)^{0.45} \\ T_1 &= T_o + 0.0481\left(\frac{u_* z_o}{\nu}\right)^{0.45}(T_2 - T_1) \\ \Rightarrow T_1 &= \frac{T_o + bT_2}{1+b} \quad \text{with} \quad b = 0.0481\left(\frac{u_* z_o}{\nu}\right)^{0.45} \end{aligned} \tag{2.9}$$

In the equation above with Karman constant $\kappa = 0.4$, ν is kinematic viscosity ($\nu = 1.5 \cdot 10^{-5}\,\mathrm{m^2 s^{-1}}$), roughness length z_o and friction velocity u_*, the temperature flux $\overline{w'\vartheta'}$ is approximated by a flux-gradient relationship with $K = u_*\kappa\Delta/2$. For humidity, the same procedure is adopted by replacing temperature with specific humidity. It should be noted that T_1 from Equation (2.8) is the temperature at the top of the viscous sublayer at $z = \delta$, while the Deardorff relation results in a temperature at height $z = z_o$.

The thickness of the viscous sublayer δ determines how effective and how fast the information is transferred from the surface to the turbulent part of the atmosphere. According to Schlichting and Gersten (1997), the depth of the viscous sublayer is given by

$$\delta = A\frac{\nu}{u_*} \tag{2.10}$$

with a large range of numerical values for A found in the literature (Table 1).

The parameter A for the Deardorff relation given in Table 1 was obtained by Equations (2.8)–(2.10):

$$\begin{aligned} a = b \quad &\Rightarrow \quad \frac{K\delta}{\nu_h \Delta} = 0.0481\left(\frac{u_* z_o}{\nu}\right)^{0.45} \\ &\Rightarrow \delta = \frac{0.0481}{\kappa}\left(\frac{u_* z_o}{\nu}\right)^{0.45}\frac{\nu_h}{u_*} \end{aligned} \tag{2.11}$$

The effects of this wide scatter of the parameter A to estimate the temperature at the top of the viscous layer, T_1, will be studied by using a boundary layer model and comparing the results against observations.

2.2 The boundary layer model

The studies presented here are restricted to an idealized homogeneous flat terrain and it is justifiable to use a simple PBL model to calculate the distribution of meteorological variables in time and height. The PBL model consists of prognostic equations for horizontal wind components, temperature including longwave radiation fluxes, humidity and turbulence kinetic energy. All turbulent fluxes are parameterized using K-theory. For a more detailed explanation, see Gross (2012, 2019).

At the upper boundary at a height of 3,000 m, an undisturbed situation is assumed, with prescribed values of 5 m/s for wind, 303 K for potential temperature, 0.006 kg/kg for specific humidity and zero turbulence kinetic energy. At the lower boundary at the height of the viscous sublayer, the wind is zero, the turbulence kinetic energy is proportional to the local friction velocity squared, temperature is determined by a surface energy budget and the specific humidity is according to Gross (1993).

Within the ground, temperature and soil water are calculated at different levels at depths of 2, 5, 10, 20, 50 and 100 cm as described by Maronga et al. (2020). In the atmosphere, a grid interval of 2 m up to 10 m height and an expanded grid above up to 3,000 m is used.

3 Results

To verify the results of this study, additional information, such as the surface temperature T_o and the thermal diffusivity ν_B of the soil, need to be derived from observations in a first step, followed by a sensitivity study on the effect of parameter A on obtaining the depth of the viscous surface layer. A final application and comparison demonstrate the great importance of δ on the daily maximum temperature, depending on the wind speed.

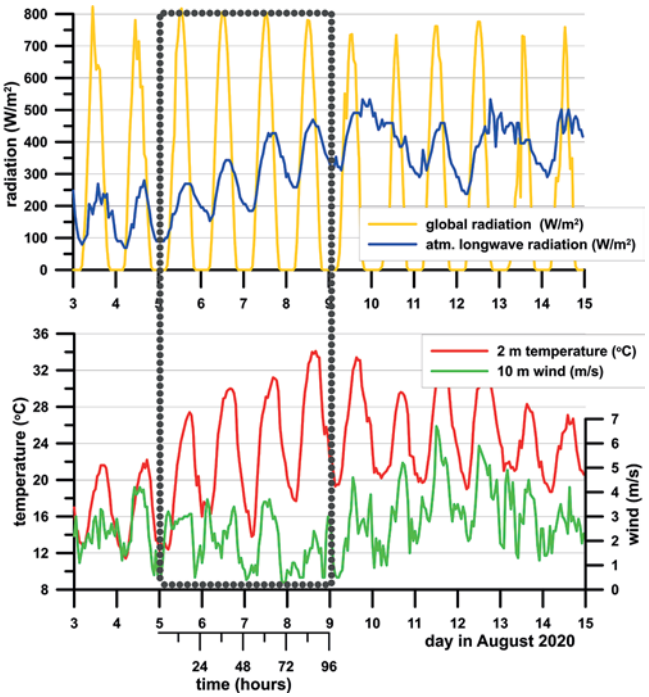

Figure 2: Observations at the DWD station Braunschweig. Selected four-day period is highlighted by the dotted box.

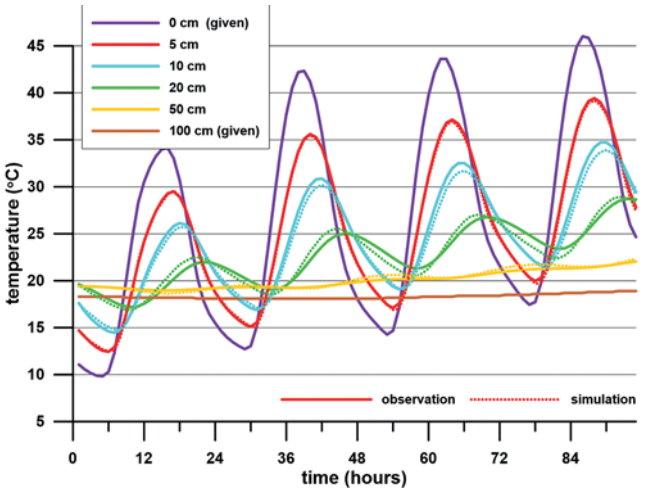

Figure 3: Observed and simulated soil temperatures at different depths.

3.1 Observations

Observations at the synoptic station Braunschweig (station ID 662) of the German Meteorological Service (DWD, 2020) are used for further studies and comparisons. This station has been selected because a wide range of parameters are available, which are necessary if the heat budget of the surface (Eq. (2.1)) is intended to be used. Besides 2-m temperature and 10-m wind, global radiation and atmospheric longwave radiation, soil temperatures as well as soil moisture (Böske, 2020) at different levels (5 cm, 10 cm, 20 cm, 50 cm and 100 cm) within the ground are available on an hourly basis. A four-day period, 5–9 August 2020, has been selected for this study (Fig. 2). During this time, an undisturbed incoming radiation heats up the ground and maximum 2-m temperatures increase continuously from 27 °C to 34 °C. In general, the wind speed is low, with higher values around 3 m/s during the day and lower nighttime values (≈ 1 m/s). Observed temperatures in the ground are given in Fig. 3. On 8 August, the soil temperature at 5 cm depth is above 39 °C.

3.2 Surface temperature

Besides the calculation of the temperature at the surface (T_o) with a surface energy budget, selected observations in combination with the heat conduction equation (Eq. (2.7)) can be used as an alternative approach. If observed temperatures within the soil at various depths are available, then the discretized Equation (2.7) for the first level in the ground reads (Liebethal and Foken, 2007)

$$\begin{aligned} \frac{T^{t+\Delta t}_{5\,\mathrm{cm}} - T^{t}_{5\,\mathrm{cm}}}{\Delta t} &= \nu_B \frac{T^{t}_{o} - 2\,T^{t}_{5\,\mathrm{cm}} + T^{t}_{10\,\mathrm{cm}}}{\Delta z_B^2} \\ \rightarrow T^{t}_{o} &= 2\,T^{t}_{5\,\mathrm{cm}} - T^{t}_{10\,\mathrm{cm}} + \frac{T^{t+\Delta t}_{5\,\mathrm{cm}} - T^{t}_{5\,\mathrm{cm}}}{\Delta t} \frac{\Delta z_B^2}{\nu_B} \end{aligned} \tag{3.1}$$

where Δz_B is the distance of the observations within the soil (here, 5 cm), Δt is a time step and ν_B is the thermal diffusivity. However, ν_B is not known for this specific period, but it may also be determined with the discretized heat conduction equation when using observed soil temperatures at three different depths and rearranging Equation (3.1). For every hour of the period, ν_B was calculated in this way and these values are used to determine a 24-hour mean. However, in order to restrict the calculated values within a realistic range, only thermal diffusivities $0.04 \cdot 10^{-6} < \nu_B < 4 \cdot 10^{-6}$ m^2/s are considered (Table 2).

The larger values of ν_B in deeper layers are caused by the composition of the soil and different soil moisture levels. The last rain before the period considered here was on 2 August. While the moisture content of the upper layer was strongly reduced day by day by evapotranspiration, the deeper part of the soil remains nearly unchanged, with values of around 10 % by volume.

For simplification and for practical use, a representative value of ν_B for the four-day period was calculated as a weighted mean for layers 1 and 2, resulting in $\nu_B = 0.62 \cdot 10^{-6}$ m^2/s. This value is on the order of realistic values known from literature (Hillel, 1998, Zmarsly et al., 2002).

Using this representative value of ν_B in Equation (3.1), the surface temperature T_o is calculated with a time step of $\Delta t = 60$ s. Finally, the success of the presented approach will be tested by solving the heat conduction equation with the prescribed T_o (calculated as

Table 2: Calculated daily mean of ν_B (10^{-6} m^2/s) for different soil layers. Number of values to estimate the daily mean are given in brackets.

layers	depths used	August 5	August 6	August 7	August 8	4-day mean
1	5-10-20 cm	0.33 (21)	0.34 (21)	0.34 (21)	0.35 (20)	0.34
2	10-20-50 cm	0.70 (22)	0.71 (21)	0.76 (21)	0.71 (20)	0.72
3	20-50-100 cm	0.79 (20)	0.93 (18)	0.96 (19)	1.04 (17)	0.93

described above) and $T_{-100\,\mathrm{cm}}$ (observed). The simulated temperature distribution within the soil layer at different levels is presented in Fig. 3. The calculated diurnal temperature variation in all depths is close to the observed variation, with mean absolute errors for the four-day period of 0.26 K (5 cm), 0.60 K (10 cm), 0.64 K (20 cm) and 0.24 K (50 cm). Based on these encouraging results it can be assumed that, in particular, the estimated surface temperature T_o is in a realistic and credible range.

3.3 Temperature at the top of the viscous sublayer

With the surface temperature T_o, estimated as described above, and the observed 2-m temperature T_2, Equation (2.8) can be used to calculate the temperature at the top of the viscous sublayer T_1 for different values of A from Table 1. For the Deardorff relation, $z_o = 0.03$ m is used and the friction velocity u_* is determined from the logarithmic wind profile with the observed 10-m wind. In order to avoid dividing by zero when calculating δ, a minimum friction velocity of $u_* = 0.01$ m/s is used. Results are presented in Fig. 4 for the four-day period considered in this study. Although the diurnal variation is very similar for all calculations, T_1 during the daytime becomes lower for larger values of A. An increasing value of A means an increasing depth of the viscous sublayer, where molecular transport is of particular importance for the transport of heat and moisture. Consequently, for larger values of δ, the temperature gradient close to the ground becomes larger. The effects of A on T_1 are demonstrated by calculating the temperature differences from a reference, for which the result for $A = 19.2$ is adopted. For values of A smaller than 5, daytime maximum temperatures are around 4 K higher than for the reference case. For increasing values of A above $A = 10$, the differences become significantly smaller. The results for the Deardorff relation with a small A ($Dd = 0.0481$) can be improved by dropping the factor of 0.74 in Equation (2.9) ($Dd = 0.065$) as suggested by Zeng and Dickinson (1998), but this still results in maximum temperature differences of about 3 K. During the night, the results are very similar because the friction velocity is small, resulting in a larger depth of the viscous sublayer in general.

As described by Foken (2002) the depth of the viscous sublayer consists of a laminar layer and a buffer zone above. In this paper, no distinction is made between these two different internal layers. This might explain the larger values of A to achieve more realistic results compared to smaller values (e.g. $A = 5$, Schlichting and Gersten, 1997).

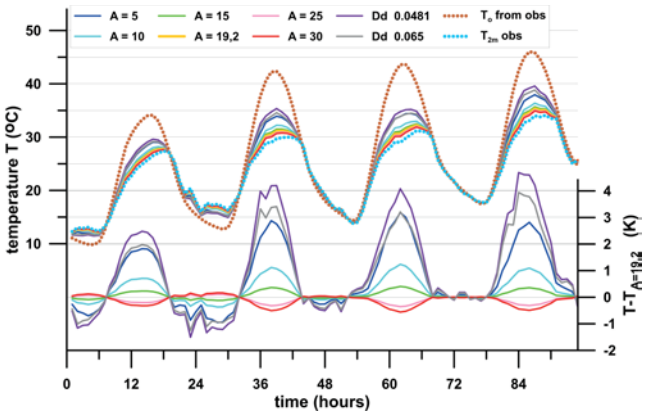

Figure 4: Calculated temperatures T_1 for different values of A (above) and temperature difference to the results of a reference run with $A = 19.2$ (below).

3.4 Soil-atmosphere simulation

In order to stay close to the observations, the PBL model introduced above is used to simulate the four-day period with specified hourly values of observed global radiation and downward longwave radiation. Between these hourly values, a linear interpolation is used. In order to find a suitable value for A to estimate the depth of the viscous sublayer and to calculate an appropriate lower boundary condition for temperature and humidity, numerous numerical simulations have been performed for different values of A. The range of parameter A was between 1 and 30 with an increment of 0.1. As a measure to evaluate the results and to quantify the errors, the mean absolute error between the observed and simulated 2-m temperatures as well as for soil temperatures at 5 cm in the ground have been calculated. The results given in Fig. 5 show a distinct minimum for both values, with the smallest error for a value of A around 19.2.

The simulated results with the coupled soil-atmosphere PBL model using a viscous sublayer depth of $\delta = 19.2\nu/u_*$ are presented in Fig. 6. Within the ground, temperatures at all depths follow the observations reasonably well. Only for the first and the last day of the four-day period does the simulated surface temperature T_o differ shortly after noon from the observed value by 2–4 K. These differences propagate into the soil, resulting in a warmer upper soil layer during the first day and a slightly cooler layer around the end of the simulation period. However, this mismatch has only a small impact on the 2-m temperature in the atmosphere. While simulated temperatures on the fourth day follow nearly perfectly the diurnal course of the observations, larger

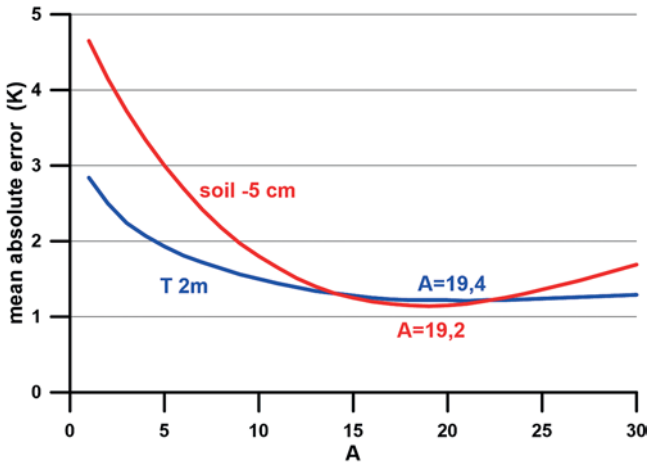

Figure 5: Mean absolute error between observed and simulated 2-m temperatures and for soil temperatures at 5 cm in the ground for different values of the parameter A.

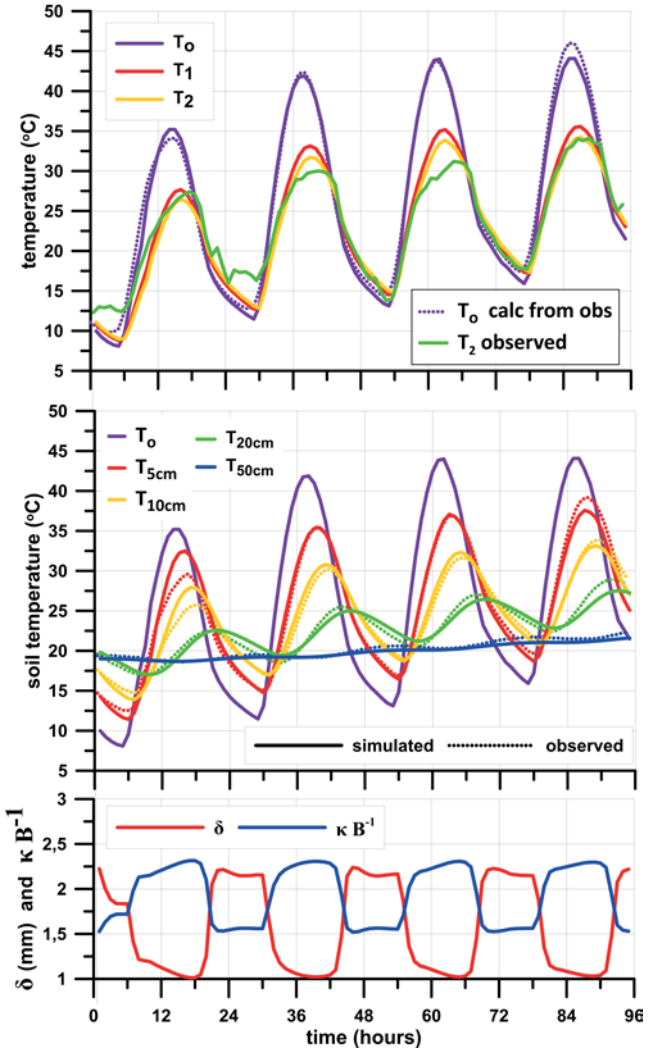

Figure 6: Diurnal variation of simulated temperatures in the lowest atmosphere (above), within the soil (middle) and for δ and κB^{-1} (below).

daytime differences around noon are obvious for the other days.

A diurnal variation of the thickness of the viscous sublayer is obvious from this figure. During the day, δ is eroded from above by enhanced turbulence, while overnight, a sublayer depth of around 2 mm is simulated. δ is the height, where the lower boundary condition for temperature is defined and therefore comparable to the thermal roughness length z_{oT}. For a comparison of the available observations with regard to z_o and z_{oT}, a quantity B^{-1} is introduced with

$$\kappa B^{-1} = \ln \frac{z_o}{z_{oT}} . \tag{3.2}$$

Garratt and Hicks (1973) summarized the findings concerning B^{-1} depending on the roughness Reynolds number $Re_* = u_* z_o/\nu$. For the range $10 < Re_* < 200$, they evaluated a typical value of $\kappa B^{-1} \approx 2$. For the meteorological situation adopted here, Re_* is between 50 and 150 and the calculated values $1.5 < \kappa B^{-1} < 2.3$ are very comparable to the values given in Garratt and Hicks (1973), Kanda et al. (2007) and Li et al. (2017).

3.5 Effects of near surface wind on daily maximum temperatures

Nighttime minimum temperatures are not very sensitive to a specific value of the parameter A in Equation (2.9) because a small value of the friction velocity, which is typical for the night, is sufficient to cause a larger depth of the viscous sublayer. However, during the daytime hours with an unstable stratification near the ground, the friction velocity is large and small differences in u_* may result in significant variations in T_1, the lower boundary condition for atmospheric temperature. In order to find out whether the relation $\delta = 19.2\nu/u_*$ is also valid for a wider range of near surface winds, a sensitivity study was conducted to find a relationship between wind speed and daily maximum 2-m temperature $T_{\max}$. For this numerical experiment, all parameters were fixed except the superimposed wind speed. The meteorological situation represents a clear summer day with strong solar radiation and therefore simulated maximum temperatures are, in general, above 30 °C (Fig. 7). The most obvious feature is a maximum of $T_{\max}$ for a 10-m wind around $u = 2.5$ m/s. For smaller values of u as well as for larger values, the maximum temperature at the 2-m level is significantly lower. This result is compared to observations at four DWD-stations in the northern part of Germany along a west-east running line from Meppen in the west to Lindenberg in the east (DWD, 2020). At these stations, daily maximum temperatures during the summer months JJA for the period 1990–2019 are evaluated together with the associated wind. The 99-percentile value for each wind speed class of 0.5 m/s was adopted as the maximum temperature and plotted in Fig. 7. For all observations of the four selected stations, there also exists a maximum of T_{max} for a wind speed around 2–3 m/s.

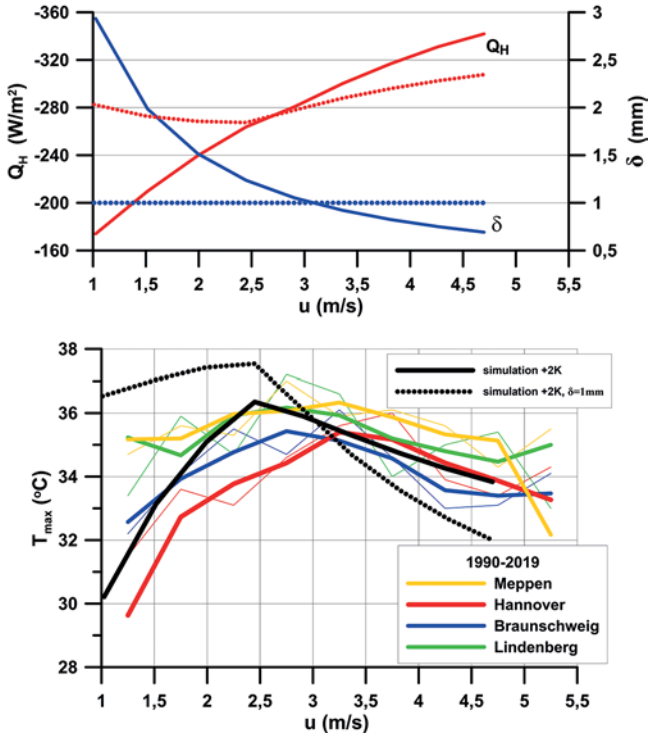

Figure 7: Top: Depth of the viscous sublayer δ and turbulent heat flux Q_H for different wind speeds for the time when T_{max} is simulated. Bottom: Daily maximum temperatures depending on wind speed. Observations: thin lines – original data, thick lines – running mean.

For a better visual comparison, a constant value of 2 K is added to the simulated temperatures presented in Fig. 7.

This specific relation between daily maximum temperature and wind speed can be explained by the two different processes that are responsible for transporting the surface heat up to the 2-m observation level. At the time when T_{max} is simulated and for low wind conditions, δ is relatively large and molecular transport is not very efficient, resulting in a large temperature gradient within the viscous sublayer, with high values of T_o and small values of T_1 at the lower boundary of the turbulent layer (Fig. 7 top). For increasing wind speed, the turbulent sensible heat flux Q_H becomes dominant, resulting in an effective transport of heat into the higher levels of the atmospheric boundary layer. This turbulent mixing of near surface warm air with a larger volume of air above then prevents higher values of T_{max}. Simulations with a constant value of $\delta = 1$ mm, which corresponds roughly to $z_o/z_{oT} \approx 10$, cannot reproduce the observations with the same quality. Especially for a smaller friction velocity, larger values of T_{max} are calculated with the assumption δ = const.

4 Conclusions

A one-dimensional boundary layer model was used to study the effects and the importance of the viscous surface layer, especially on the temperature near the ground. While at the lower boundary the condition for wind can be well specified at a roughness height, this height is not appropriate for temperature as well. A reasonable explanation for this fact is caused by the different physical mechanisms for heat and momentum transfer very close to the ground. While the heat flux is mainly controlled by heat conduction, the form drag determines the momentum flux.

Questions remain on whether an appropriate lower boundary condition for temperature in the turbulent boundary layer can be determined using available information, such as surface radiation temperature, and the observed or simulated data, e.g., at 2 m height in the atmosphere. Usually, the required temperature is expressed as a weighted mean of these two values. One weighting factor is the depth of the viscous surface layer δ, which determines the effectiveness of molecular heat transfer from the ground up to the height where turbulence takes over the heat flux into the atmosphere.

It is known that δ depends on friction velocity, molecular thermal diffusivity and an empirical factor for which a wider range of values are published in the literature. In this paper, an optimized empirical factor A is calculated in such a way that temperatures in the atmosphere as well as in the ground can be reproduced with high accuracy. It is also demonstrated that the variables and parameters that are necessary for such an estimation can be deduced from observations as well.

The results of a numerical simulation for a four-day period with an optimized A show very good agreement with the observed temperatures at 2 m height in the atmosphere as well as at different depths inside the ground. This is largely due to the calculation of a realistic surface temperature, which in turn depends on the diurnal variation of the depths of the viscous surface layer. During the night, δ is on the order of 2 mm, while a daytime value of around 1 mm is calculated.

The great importance of the viscous sublayer depths, depending on the time of the day, becomes particularly apparent in a final test, where the daily maximum temperature T_{max} is calculated for different wind speeds. Long term observations at various DWD stations show a pronounced maximum of T_{max} for an observed 10-m wind between 2–3 m/s, with a strong decrease for a lower wind speed and a weaker decrease towards larger values. This correlation of T_{max} and wind speed, and therefore friction velocity u_*, can be directly attributed to the thickness of the viscous sublayer. For low values of u_* the thickness is large and heat transfer by molecular diffusion from the ground up to a height where turbulence is effective is small. Consequently, the 2-m maximum temperature benefits to a lesser degree from the high surface temperature. For increasing friction velocity, δ decreases and the turbulent sensible heat flux becomes very efficient at transporting warm air from the ground into the atmosphere. This process reduces the surface temperature and, due to an effective mixing with the air in the PBL, also reduces T_{max}. With a constant value of δ, which can be compared to a thermal rough-

ness length, the observations with regard to T_{max} cannot be reproduced with a similar quality.

Based on the results presented in this paper the author recommends to consider a time-dependent viscous surface layer of variable depth in high resolution PBL models (e.g. PALM-4U, Maronga et al., 2020) for a sophisticated formulation of especially the lower boundary condition for temperature.

Acknowledgements

The publication of this article was funded by the Open Access Fund of Leibniz University Hannover.

References

Beljaars, A.C.M., A.A.M. Holtslag, 1991: Flux parameterization over land surfaces for atmospheric models. – J. Appl. Meteor. **30**, 327–341.

Böske, L., 2020: personal communication. – DWD Braunschweig.

Chen, F., Z. Janjic, K. Mitchell, 1997: Impact of atmospheric surface-layer parameterizations in the new land-surface scheme of the NCEP mesoscale eta model. – Bound.-Layer Meteor. **85**, 391–421.

Chriss, T.M., D.R. Caldwell, 1984: Universal similarity and the thickness of the viscous sublayer at the ocean floor. – J. Geophys. Res. **89**, 6403–6414.

Deardorff, J.W., 1974: Three-dimensional numerical study of the height and mean structure of a heated planetary boundary layer. – Bound.-Layer Meteor. **7**, 81–106.

DWD, 2020: open data. – https://opendata.dwd.de/climate_environment/CDC/observations_germany/climate/hourly/solar/

Foken, Th., 2002: Some aspects of the viscous sublayer – Meteorol. Z. **11**, 267–272.

Garratt, J.R., 1992: The atmospheric boundary layer. – Cambridge University Press, 316 pp.

Garratt, J.R., B.B. Hicks, 1973: Momentum, heat and water vapour transfer to and from natural and artificial surfaces. – Quart. J. Roy. Meteor. Soc. **99**, 680–687.

Gross, G., 1993: Numerical simulation of canopy flows. – Springer Verlag Berlin, 167 pp.

Gross, G., 2012: Numerical simulation of greening effects for idealised roofs with regional climate forcing. – Meteorol. Z. **21**, 173–181.

Gross, G., 2019: On the self-ventilation of an urban heat island. – Meteorol. Z. **28**, 87–92.

Hillel, D., 1998: Environmental soil physics. – Academic Press, New York, 771 pp.

Janjic, Z.I., 1994: The step-mountain eta coordinate model: Further developments of the convection, viscous sublayer, and turbulence closure scheme. – Mon. Wea. Rev. **122**, 927–945.

Janjic, Z.I., 2019: The surface layer parameterization in the NMM models. – Office note 497, DOI:10.25923/9qej-k604, NOAA Maryland.

Kanda, M., M. Kanega, T. Kawai, R. Moriwaki, H. Sugawara, 2007: Roughness lengths for momentum and heat derived from outdoor urban scale models. J. Appl. Meteor. Climatol. **46**, 1067–1079.

Li, D., A. Rigden, G. Salvucci, H. Liu, 2017: Reconciling the Reynolds number dependence of scalar roughness length and laminar resistance. – Geophys. Res. Lett. **44**, 3193–3200.

Liebethal, C., Th. Foken, 2007: Evaluation of six parameterization approaches for the ground heat flux. – Theor. Appl. Climatol. **88**, 43–56.

Liu, W.T., K.B. Katsaros, J.A. Businger, 1979: Bulk parameterization of air-sea exchange of heat and water vapor including the molecular constraints at the interface. – J. Atmos. Sci. **36**, 1722–1735.

Mahrt, L., 1996: The bulk aerodynamic formulation over heterogeneous surfaces. – Bound.-Layer Meteor. **78**, 87–119.

Maronga, B., S. Banzhaf, C. Burmeister, T. Esch, R. Forkel, D. Fröhlich, V. Fuka, K.F. Gehrke, J. Geletic, S. Giersch, T. Gronemeier, G. Gross, W. Heldens, A. Hellsten, F. Hoffmann, A. Inagaki, E. Kadasch, F. Kanani-Sühring, K. Ketelsen, B.A. Khan, C. Knigge, H. Knoop, P. Krc, M. Kurppa, H. Maamari, A. Matzerakis, M. Mauder, M. Pallasch, D. Pavlik, J. Pfafferott, J. Resler, S. Rissmann, E. Russo, M. Salim, M. Schrempf, J. Schwenkel, G. Seckmeyer, S. Schubert, M. Sühring, R. von Tils, L. Vollmer, S. Ward, B. Witha, H. Wurps, J. Zeidler, S. Raasch, 2020: Overview of the PALM model system 6.0. – Geosci. Model Dev. **13**, 1335–1372.

Pielke, R.A., 2002: Mesoscale meteorological modeling. – Academic Press, San Diego, 676 pp.

Schlichting, H., K. Gersten, 1997: Grenzschicht-Theorie. – Springer Verlag Berlin, 851 pp.

Stull, R.B., 1988: An introduction to boundary layer meteorology. Kluwer Academic, 666 pp.

Sun, J., S.K. Esbensen, L. Mahrt, 1995: Estimation of surface heat flux. – J. Atmos. Sci. **52**, 3162–3171.

Zeng, X., R.E. Dickinson, 1998: Effect of surface sublayer on surface skin temperature and fluxes. – J. Climate. **11**, 537–550.

Zilitinkevich, S.S., 1995: Non-local turbulent transport: Pollution dispersion of coherent structure of convective flows. – In: H. Power, N. Moussiopoulos, C.A. Brebbia (Eds.): Air pollution III – Volume I. Air pollution theory and simulation. – Computational Mechanics Publications, Southampton, Boston, 53–60.

Zmarsly, E., W. Kuttler, H. Pethe, 2002: Meteorologisch-klimatologisches Grundwissen. – Ulmer Verlag, 176 pp.